CT&F - Ciencia, Tecnología y Futuro - Vol. 6 Num. 2 Dec. 2015 Pag. 45 - 56

JOURNAL
CIENCIA, TECNOLOGÍA Y FUTURO

ISSN (Print) 0122-5383
ISSN (Online) 2382-4581

IX Simposio Colombiano de Catálisis (SiCCat)+

Journal of oil, gas and alternative energy sources

ETHYL ACETATE OXIDATION OVER MnO_x-CoO_x. RELATIONSHIP BETWEEN OXYGEN AND CATALYTIC ACTIVITY

OXIDACIÓN DEL ACETATO DE ETILO SOBRE MnO_x-CoO_x. RELACIÓN ENTRE OXÍGENO Y ACTIVIDAD CATALÍTICA

OXIDAÇÃO DO ACETATO DE ETILO SOBRE MnOx -CoOx . RELAÇÃO ENTRE OXIGÊNIO E ATIVIDADE CATALÍTICA

María-Haidy Castaño-Robayo[1], Rafael Molina-Gallego[1] and Sonia Moreno-Guáqueta*[1]

[1]Estado Sólido y Catálisis Ambiental (ESCA), Departamento de Química, Facultad de Ciencias, Universidad Nacional de Colombia, Bogotá, Cundinamarca, Colombia

e-mail: smorenog@unal.edu.co

(Received: Sep. 28, 2015; Accepted: Dec. 02, 2015)

ABSTRACT

Catalytic oxidation is an alternative for the transformation of volatile organic compounds. *Mn* and *Co* catalysts are the most active in oxidation reactions because of their redox properties and oxygen mobility. Co-precipitation is one of the methods most used to prepare metal oxides. In this regard and in order to understand the relationship between oxygen species and the activity of the catalysts, in this work mixed oxides of *Co-Mn-Mg-Al* were prepared by the co-precipitation method. The catalysts were characterized by XRD, surface area, temperature-programmed desorption of oxygen, oxygen storage capacity, $^{18}O/^{16}O$ isotopic exchange; and the catalytic activity was evaluated in the oxidation of ethyl acetate. The results indicate that manganese-containing oxides have surface adsorbed oxygen and a greater amount of oxygen susceptible to redox cycles while oxides containing cobalt show high oxygen mobility. In the oxidation of ethyl acetate, the most labile oxygens undergo redox cycles and surface adsorbed oxygens are the species involved.

Keywords: *Hydrotalcite, Mixed oxide, Mobility, Oxygen storage capacity.*

How to cite: Castaño-Robayo, M. H., Molina-Gallego, R. & Moreno-Guáqueta, S. (2015). Ethyl acetate oxidation over MnO_x-CoO_x. Relationship between oxygen and catalytic activit. *CT&F - Ciencia, Tecnología y Futuro,* 6(2), 45-56.

**To whom correspondence should be addressed*

+IX Simposio Colombiano de Catálisis (SiCCat) y III Escuela Colombiana de catálisis, Universidad del Vallle, Colombia, September 7-11, 2015.

RESUMEN

La oxidación catalítica es una alternativa promisoria para la transformación de contaminantes atmosféricos como los compuestos orgánicos volátiles. Los catalizadores basados en óxidos de *Mn* y *Co* se encuentran dentro de los más activos en las reacciones de oxidación debido a sus propiedades redox y su movilidad de oxígeno. La co-precipitación es uno de los métodos más empleados para preparar óxidos metálicos por las propiedades únicas que presentan los sólidos finales. En tal sentido y con el fin de comprender la relación existente entre las especies de oxígeno y la actividad de los catalizadores, en éste trabajo se prepararon óxidos mixtos de *Mn-Co-Mg-Al* mediante la metodología de coprecipitación. Los catalizadores se caracterizaron por difracción de rayos X, área superficial, desorción de oxígeno a temperatura programada, capacidad de almacenamiento de oxígeno e intercambio isotópico $^{18}O/^{16}O$; adicionalmente, se evaluó la actividad catalítica en la oxidación del acetato de etilo. Los resultados indican que los óxidos que contienen manganeso presentan especies de oxígeno adsorbidas superficialmente y una mayor cantidad de oxígenos susceptibles de sufrir ciclos redox mientras que los óxidos que contienen cobalto demuestran la presencia de oxígenos con mejor movilidad. En la oxidación del acetato de etilo, los oxígenos más disponibles de conducir ciclos redox y los oxígenos adsorbidos en la superficie resultan ser el factor determinante.

Palabras clave: *Hidrotalcita, Óxido mixto, Movilidad, Capacidad de almacenamiento de oxígeno.*

RESUMO

A oxidação catalítica é uma alternativa promissória para a transformação de contaminantes atmosféricos como os compostos orgânicos voláteis. Os catalizadores baseados em óxidos de *Mn* e *Co* se encontram dentro dos mais ativos no que tange as reações de oxidação por conta de suas propriedades redox e sua mobilidade de oxigênio. A co-precipitação é um dos métodos mais utilizados para preparar óxidos metálicos graças às propriedades únicas exibidas pelos sólidos finais. Nesse sentido e no intuito de compreender a relação existente entre as espécies de oxigênio e atividade dos catalizadores, neste trabalho preparamos óxidos mistos de *Mn-Co-Mg-Al* mediante a metodologia de co-precipitação. Os catalizadores se caracterizaram pela difração de raios X, área superficial, dessorção de oxigênio a temperatura programa, capacidade de armazenamento de oxigênio e intercâmbio isotópico $^{18}O/^{16}O$; além disso, a atividade catalítica na oxidação do acetato de etilo também foi avaliada. Os resultados indicam que os óxidos que contém manganês apresentam espécies de oxigênio adsorvidas superficialmente e uma maior quantidade de oxigênios suscetíveis de sofrer ciclos redox enquanto os óxidos que contêm cobalto apresentam oxigênios com melhor mobilidade. Na oxidação do acetato de etilo, os oxigênios mais disponíveis para a condução de ciclos redox e os oxigênios adsorvidos na superfície são o fator determinante.

Palavras-chave: *Hidrotalcita, Óxido misto, Mobilidade, Capacidade de armazenamento de oxigênio.*

1. INTRODUCTION

It has been reported that the adsorbed oxygen species on the surface defects together with the lattice oxygens with high mobility are responsible for the oxidation reactions on metallic oxides (Moro-oka, Ueda & Lee, 2003). In the oxidation of propene on *CoCe* oxides a direct relation between the redox properties and the catalytic behavior was found due to the high oxygen mobility present in these solids. On a *Ce* single oxide the adsorbed oxygen species on surface vacancies are involved (Liotta *et al*., 2008). Likewise, in the oxidation of propane on a *MnNi* catalyst a high activity is observed due to the presence of surface oxygen species (denominated α) while in the oxidation of ethanol a *MnFe* catalyst exhibits the best catalytic by the participation of lattice oxygens (denominated β), which play an important role in the process (Morales, Barbero & Cadús, 2007).

Regarding mixed *Mn* and *Co* oxides derived from hydrotalcite type precursors, there is scarce information about the oxygen species involved in the oxidation of Volatile Organic Compounds (VOCs). This work focuses on studying the species of oxygens present in these materials employing the techniques of temperature-programmed desorption of oxygen (O_2-TPD), Oxygen Storage Capacity (OSC) and $^{18}O/^{16}O$ isotopic exchange in order to establish a correlation between these species and the catalytic behavior.

2. THEORETICAL FRAME

VOCs can be defined as "those organic compounds which at a temperature of 20°C present a vapor pressure of 0.01 kPa or superior or a volatility equivalent to the particular conditions of use" (Garetto, Legorburu & Montes, 2008).

The abatement of VOCs is of great importance since their emission is hazardous to the environment and human health. The VOCs are involved in the formation of "photo-chemical smog", some are toxic, carcinogenic or teratogenic and many of them are connected to the greenhouse effect (Koppmann, 2010).

Thermal and catalytic oxidation are the most efficient methods to eliminate VOCs emission (~99%). However, thermal oxidation requires a high operating temperature consuming significant amounts of energy and producing high levels of nitrogen oxides (*NOx*). Catalytic oxidation reduces the oxidation temperatures and, in consequence, generates a smaller quantity of *NOx* (Khan & Ghoshal, 2000).

Metallic oxides are among the materials most used in the catalytic oxidation due to their great electronic mobility and high resistance to deactivation by their high surface areas (Garetto *et al*., 2008; Spivey, 1987). A common characteristic of metallic oxides in the oxidation of VOCs is the presence of multiple states of oxidation, which enables the formation of redox cycles where the metal is reduced by the VOC and re-oxidized by the oxygen of the current.

Manganese and cobalt oxides are promising catalysts in oxidation reactions since they show a high capacity to form oxides in different states of oxidation, elevated capacity of oxygen storage and a optimum strength of the M-O bond (Fierro, 2006; Liotta *et al*., 2013).

Many synthesis methods have been employed for the preparation of metallic oxides (Avgouropoulos, Ioannides & Matralis, 2005; Schwarz, Contescu & Contescu, 1995; Zhu *et al*., 2010). Co-precipitation is one of the most widely used methods for the synthesis of catalyst from the generation of hydrotalcites as precursors of mixed oxides. The final products show characteristics such as homogeneous distribution, good dispersion of the components and a high surface (Cavani, Trifirò & Vaccari, 1991; Vaccari, 1998).

Layered Double Hydroxides (LDH) also known as anionic clay or Hydrotalcite Type (HT) represent a kind of synthetic laminar materials whose general formula could be expressed as $[M^{2+}_{1-x}M^{3+}_{x}(OH)_2]^{x+}[A^{n-}_{x/n}\ mH_2O]^{x-}$, where M^{2+} and M^{3+} represent divalent and trivalent cations respectively, A^{n-} an anion and x which must be found in the interval between 0.2 and 0.33 to preserve the structure; if x is out of this range, hydroxides and other compounds can be formed (Kovanda & Jirátová, 2011; Xu *et al*., 2011).

The hydrotalcite structure is related to that of brucite $Mg(OH)_2$ where the Mg^{2+} is octahedrally coordinated with six hydroxile groups and the octahedrons generated

share their sides to form bi-dimensional layers, which stay joined by Van der Waals forces. The replacement of some cations for example Mg^{2+} for Al^{3+}, creates positive charges that are compensated for by the presence of anions in the interlayer spacing forming the hydrotalcite structure.

The Mn^{2+} and Co^{2+} cations are capable of completely or partially replacing the Mg^{2+} ions within the laminar structure forming LDH materials of different compositions. The thermal decomposition of the hydrotalcites allows us to obtain mixed oxide with important industrial applications involving the use of catalysts (Xu *et al*., 2011).

3. EXPERIMENTAL

Catalysts Synthesis

Solutions of the respective nitrates were used maintaining the ratios $M^{2+}/M^{3+} = 3$, $M^{2+}/Mg^{2+} = 1$ (where $M = Mn^{2+}$, Co^{2+} or $Mn^{2+}+Co^{2+}$). For the *Mn* and *Co* oxide the ratio $Co^{2+}/Mn^{2+} = 0.5$ was preserved. The Mg^{2+}, Al^{3+}, Mn^{2+} and/or Co^{2+} nitrates were mixed and added dropwise to a solution 0.2 M of K_2CO_3 with constant stirring, maintaining pH level between 9.5 and 10.5 (addition of a solution of *NaOH* 1 M). The precipitate obtained was aged for 18 h without stirring. Subsequently, all the solids obtained were washed and dried at 60°C in air for 18 h to obtain the respective hydrotalcite type precursors denominated HTMn1.0, HTCo1.0 and HTCoMn0.5.

The hydrotalcites were calcined at 500°C for 16 h to generate the respective mixed oxides denominated CPMn1.0, CPCo1.0 and CPCoMn0.5 (were CP indicate co-precipitation).

Characterization

X Ray Diffraction

The X ray patterns were taken with a Panalytical X´Pert PRO MPD diffractometer equipped with a copper anode (λ = 1.5406 Å) and using a velocity of 1°θ·min^{-1} and a step size of 0.02°θ.

N_2 Adsorption

Micromeritics® ASAP 2020 equipment was used. The samples were degassed at 350°C for 4 hours and then the N_2 adsorption-desorption isotherms were carried out at -196°C.

Temperature-Programmed Desorption of Oxygen (O_2-TPD)

The mixed oxides (0.100 g) were degassed at 400°C for 1 h in the presence of *He*. The adsorption of O_2 (9.99% O_2 in *He*) was carried out at 400°C and at room temperature under the same atmosphere 1 h for each temperature. A flux of 50 mL·min^{-1} of *He* was used to remove the excess O_2 and finally desorption of the O_2 was carried out by increasing the temperature on a heating ramp of 10ºC·min^{-1} to 900°C. Origin®Pro 8.5 software was used to quantify the areas associated with desorption of O_2.

Oxygen Storage Capacity (OSC)

The analyses were conducted using equipment built by the ESCA group employing the H_2/O_2 pulse injection technique (Christou *et al*., 2012). Prior to carrying out the measurements, samples (0.015 g in 0.100 g of *SiC*) were pre-oxidized under an air flow of 10 mL·min^{-1} (21% O_2) at 400°C for 40 min and with a subsequent argon step until the $^{16}O_2$ signal was not detected. Later, the samples were cooled to 200°C under an argon flow (10 mL·min^{-1}) and alternating pulses of H_2-O_2 of 50 µL each were carried out completing two cycles. In order to know the quantity of oxygen most available to the solids in a range of temperatures, the same procedure was applied at temperatures close to 275, 345 and 400°C. The concentrations of the H_2, O_2, H_2O, *Ar* and *He* gases were monitored by mass spectrometry (Omnistar mass spectrometer) following the signals m/z = 2, 32, 18, 40 and 4, respectively.

The OSC was calculated based on the quantity of oxygen consumed during the re-oxidation stage after carrying out the H_2 pulses, and these are expressed in terms of µmol O_2·g^{-1} of catalyst. Origin®Pro 8.5 software was used to quantify the areas of each of the pulses associated with the O_2 signal.

$^{18}O/^{16}O$ Isotopic Exchange

The samples (0.030 g with 0.100 g of *SiC*) were treated under an air flow (10 mL·min^{-1}) at 400°C for 1 h. Then, cooling was permitted to 200°C under an argon flux. Pulses of 20 µmL $^{18}O_2$ were carried out on the samples at 200, 260, 330 and 400°C in presence of an argon flow (10 mL·min^{-1}). Gas composition was monitored by mass spectrometry (Omnistar mass spectrometer) following the signals m/z = 36, 34 and 32 corresponding to $^{18}O_2$, ^{18}O ^{16}O and $^{16}O_2$, respectively.

Origin®Pro 8.5 software was used to quantify the areas below the signals associated with the concentration of $^{18}O_2$, $^{18}O\ ^{16}O$ and $^{16}O_2$.

Catalytic Activity: Oxidation of Ethyl Acetate

A fixed bed reactor at atmospheric pressure in the temperature range of 400 to 150°C was used in the catalytic evaluation. Samples (0.200 g sieved < 250 µm) were pretreated in an air flux (21% O_2) at 400°C for 1 hour. The conversion curves were obtained by cooling at 1.5°C·min^{-1} from 400 to 150°C maintaining a total flow of 280 mL·min^{-1} of air with 1000 ppm of ethyl acetate. Reaction products and reactives were analyzed in line with a Shimadzu GC-17A gas chromatograph, and CO_2 production, by a Bacharach Model 3150 CO_2 analyzer equipped with an IR detector.

CO_2 conversion was calculated following the stoichiometry of the reaction and employing the following expression:

$$\%\ Yield\ to\ CO_2 = \frac{[CO_2]_{outlet}}{4 * [ethyl\ acetate]_{inlet}} * 100 \qquad (1)$$

4. RESULTS

Precursors of Mixed Oxides

The diffraction patterns of the manganese and cobalt hydrotalcites, HTMn1.0, HTCo1.0 and HTCoMn0.5 are presented in Figure 1 where they are compared to the diffractogram typical of a *Mg-Al* hydrotalcite (HTMgAl). The presence of intense signals at 11.3, 22.6 and 34.4 °2θ in the XRD patterns indicates the formation of a well crystallized laminar structure with 3R symmetry in all cases (Tsyganok & Sayari, 2006).

For HTCo1.0 the only phase identified corresponds to the hydrotalcite phase (JCPDS 70-2151) without observing any other phases associated to cobalt, which suggests its homogeneous incorporation in the hydrotalcite structure.

HTMn1.0 reveals the signals of the hydrotalcite of reference (HTMgAl) and signals attributed to hausmanite phase Mn_3O_4 (JCPDS 24-0734), rhodochrosite $MnCO_3$ (JCPDS 44-1472) and possible formation of $Mn(OH)_2$ phase (JCPDS 73-1604. Formation of Mn_3O_4 occurs for the oxidation Mn^{2+} to Mn^{3+} in the synthesis conditions. Presence of $Mn(OH)_2$ and $MnCO_3$ phases has been reported in *Mn* hydrotalcites with $Mn_xMg_{3-x}AlO$ formula (x varies in the range of 0 to 3), suggesting that at least 37.5% of the *Mg* and *Al* ions can be isomorphically substituted by the *Mn* in the hydrotalcite (Lamonier *et al*., 2007; Li *et al*., 2010; Velu *et al*., 1999).

For HTCoMn0.5 hydrotalcite signals are evidenced together with the $MnCO_3$ phase and in a lesser proportion Mn_3O_4 phase. A greater and more intense number of signals are observed for the $MnCO_3$ phase due to the presence of *Co* within the laminar structure. This result can be explained in terms of the ionic radii of the *Co*, *Mn* and the *Mg* where the Co^{2+} and the Mg^{2+} present similar ionic radii (0.65Å and 0.72 Å respectively) compared to that of the Mn^{2+} (0.83Å) which allows for the Co^{2+} to be incorporated more easily in the structure and leaves more Mn^{2+} species available to react with the carbonates and produce more $MnCO_3$ (Lamonier *et al*., 2007; Xu *et al*., 2011).

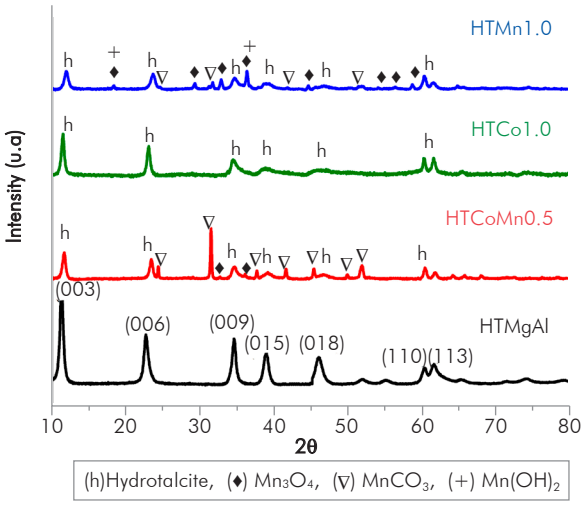

Figure 1. XRD profiles of the precursors of mixed oxides.

Mixed Oxides

It has been widely reported that the thermal decomposition of *Mg-Al* hydrotalcites begins with the loss of water molecules in the interlayers at 150-200°C, followed by the collapse of the hydroxile layers in the temperature range of 300-400°C and, finally, the complete loss of the laminar structure over 500°C (Tsai *et al*., 2011). Figure 2 shows the diffraction patterns of the manganese, cobalt and

manganese-cobalt oxides generated from the thermal decomposition of the corresponding hydrotalcite at 500°C for 16 h. The profiles do not reveal signals associated with the hydrotalcite phase, confirming the total destruction of the laminar structure and the formation of the corresponding mixed oxides.

All the mixed oxides reveal signals of the periclase phase (*MgO*). Additionally, CPMn1.0 shows peaks attributed to the presence of manganese spinels, Mn_3O_4 (JCPDS 70-2151), $MnAl_2O_4$ (JCPDS 029-0880) and Mg_2MnO_4 (JCPDS 19-0773).

In the case of oxide CPCo1.0, the phases of type $CoAl_2O_4$, Co_2AlO_4 and Co_3O_4 (JCPDS 044-0160; JCPDS 030-0814; JCPDS 042-1467 respectively) could be present. Due to the amplitude of the signals and the complexity of the peaks in the oxide mixed diffratograms it is impossible to assign the signals to a specific phase.

CPCoMn0.5 exhibits the same signals as the manganese and cobalt oxides with the possible formation of solid solutions of the $Mn_{3-x}Co_xO_4$ type (x =0 to 3) (Bordeneuve *et al.*, 2009; Jang, Wang & Chiang, 1998). Taking into account that for the synthesis of CPCoMn0.5 a ratio $Co/Mn = 0.5$ was used where the *Mn* is in a greater proportion, the possible formation of the hausmanite phase (Mn_3O_4) is to be expected with the isomorphic substitution of *Mn* for *Co* within the structure to form a solid solution of the $Mn_{3-x}Co_xO_4$, type, which would explain the similarity of the diffraction profiles of CPCoMn0.5 and CPMn1.0.

The N_2 adsorption-desorption isotherms of the mixed oxides are shown in Figure 3a. All oxides reveal type II isotherms characteristic of macro-porous materials. The presence of an H1 hysteresis loop evidences the presence of pores with uniform sizes and forms in the materials. The specific area is attributed to the formation of pores resulting from the destruction of the laminar spaces following the calcination (loss of water and carbonates) (Aguilera *et al.*, 2011). The area values determined by means of the BET model for CPMn1.0, CPCo1.0 and CPCoMn0.5 corresponding to 186, 154 and 162 $m^2 \cdot g^{-1}$, respectively. The lower value in area of solids CPCo1.0 and CPCoMn0.5 can be attributed to the formation of the spinels with the aluminum, as shown by the XRD

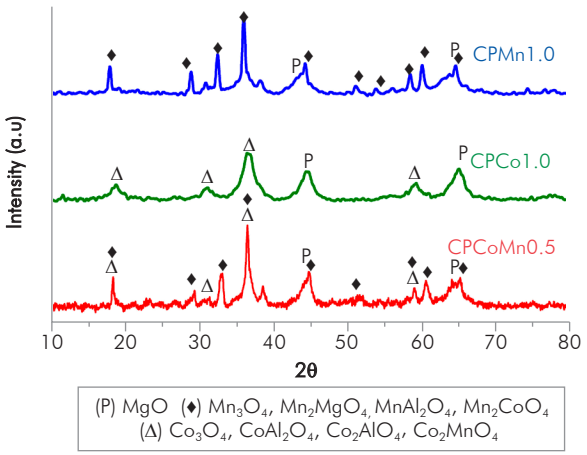

Figure 2. Diffraction patterns of the mixed oxides obtained at 500°C.

analysis, which reduce the textural properties (Mo *et al.*, 2003; Muñoz, Moreno & Molina, 2012).

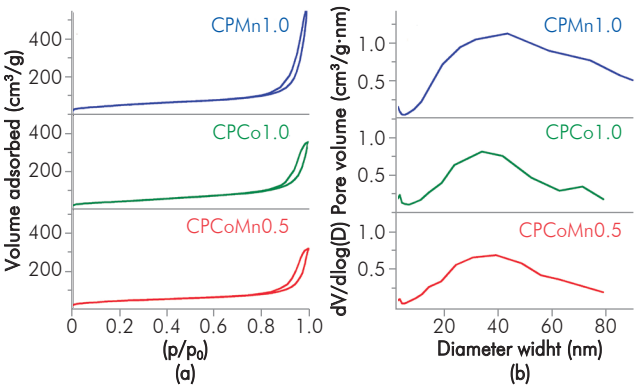

Figure 3. (a) Adsorption-desorption isotherms (b) distribution of pore size of the mixed oxides obtained by co-precipitation.

The distribution of the pore size of the oxides is presented in Figure 3b. A wide range of pore sizes from 5 to 90 nm approximately is observed in all the oxides, confirming the meso and macro-porous character of these materials.

The O_2-TPD analyses study the oxygen species involved in oxidation reactions. Desorption of oxygen species based on the temperature is carried out by means of the following process:

$O_{2(ad)} \rightarrow O^-_{2(ad)} \rightarrow O^-_{(ad)} \rightarrow O^{2-}_{(bulk)}$, where the desorption signals at temperatures lower than 400°C ascribed to oxygen species (α) like O^{2-} and O^- which are weakly linked at the surface, whereas the signals that appear

at temperatures greater than 400°C are assigned to lattice oxygens (β) which are found in diverse chemical environments (Liotta *et al*., 2008; Xue *et al*., 2007). The O_2-TPD profiles of the mixed oxides CPMn1.0, CPCo1.0, and CPCoMn0.5 are shown in Figure 4.

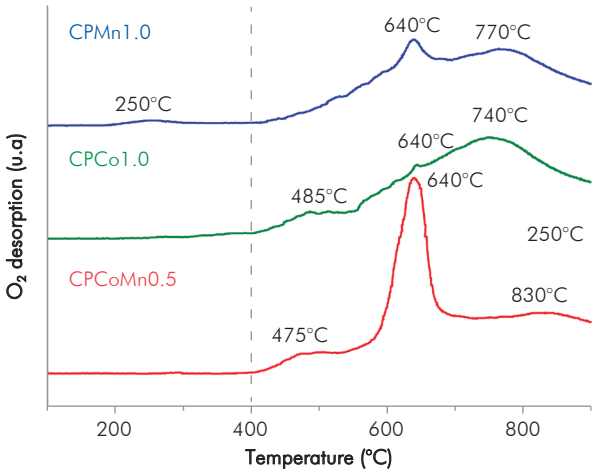

Figure 4. O_2-TPD profiles of the mixed manganese and cobalt oxides.

CPMn1.0 shows a desorption peak centered at 250°C (species α) showing that this oxide has an important concentration of surface oxygen species. The signal at 244°C has been attributed to the desorption of oxygen species of the Mn_3O_4 phase (Arnone *et al*., 1998), a temperature very close to that found in CPMn1.0 indicating the presence of the hausmanite in this oxide as was evidenced by XRD. Also, this solid presents different desorption signals at T > 400°C which correspond to lattice oxygens (species β) with different chemical environments or different oxygen mobility (Santos *et al*., 2009).

In the profile of CPCo1.0 different signals are observed in the temperature range of 400 - 900°C, which can be assigned to bulk oxygen species with different bond strength or oxygen mobility. The signal at 700°C can be attributed to the thermal decomposition of the Co_3O_4 to *CoO* (Liotta *et al*., 2008).

Mixed oxide CPCoMn0.5, exhibits signals at temperatures greater than 400°C very similar to those found in CPMn1.0 and CPCo1.0. The absence in this oxide of the signal at ~250°C characteristic of the Mn_3O_4 phase can indicate the partial substitution of the *Mn* by *Co* in the structure of the hausmanite. Likewise, the great intensity of the peak to 640°C in CPCoMn0.5 suggests that the oxygen adsorbed species fill the internal vacancies created by the substitution of *Co* by *Mn* (Merino *et al*., 2005). This results evidence the formation of a solid solution of *Co-Mn,* which leads to a cooperative effect between the phases, increasing oxygen mobility in CPCoMn0.5 as compared to CPMn1.0 oxide.

It is well known that the catalyst used in oxidation must have a large number of sites capable of linking with the oxygen molecules and also, that have a great ability to donate and accept electrons (Oyama, 1996).

Regarding mixed oxides the redox process can be described in terms of the following general mechanism:

$$\text{Cat-O} + \text{Red} \rightarrow \text{Cat} + \text{Red-O}$$

$$\text{Cat} + \text{Ox-O} \rightarrow \text{Cat-O} + \text{Ox}$$

The catalyst (Cat-O) is reduced by the substrate (reducer), which is subsequently re-oxidized by an oxidizer (Ox-O) to its initial state. The net result is the transference of oxygen to one species or another, which in the specific case of VOCs, is carried out by the oxidation of the organic compound and the reduction of the surface of the oxide due to the loss of surface oxide ions and the subsequent re-oxidation of the catalyst (Fierro, 2006).

A commonly accepted mechanism in oxidation reactions is the redox mechanism known as Mars Van Krevelen (Mars & van Krevelen, 1954; Vedrine, Coudurier, & Millet, 1997). Considering this mechanism a oxidation catalyst requires a redox couple that enables the electronic transference and also exhibit a high oxygen mobility which assures re-oxidation of the reduced catalyst.

For studying the most labile or reactive oxygen species that can participate in oxidation reactions and determine the redox ability of the *Mn* and mixed oxides, which simulates the transfer of electrons in the oxidation mechanism of VOCs, we used the OSC technique.

Figure 5 shows the OSC of the mixed oxides under dynamic conditions at different temperatures (200-400°C). The OSC increases with the rise of the temperature since at low temperatures (below 300°C) the surface and near-surface oxygen makes major

contribution to OSC and at higher temperatures (above 300°C) bulk oxygen migration plays an important role to determine the OSC performance (Wang *et al*., 2011; Zhao, Shen & Wang, 2007).

Figure 5 shows that the manganese-containing oxides exhibit OSC values greater than CPCo1.0 being CPCoMn0.5 the one that presents the most important values. This result is attributed mainly to the incorporation of *Co* in the structure of the manganese oxide (CPMn1.0) that can increase the migration of the bulk oxygen generating vacancies which form very weak bonds with the oxygen species (Wang *et al*., 2011).

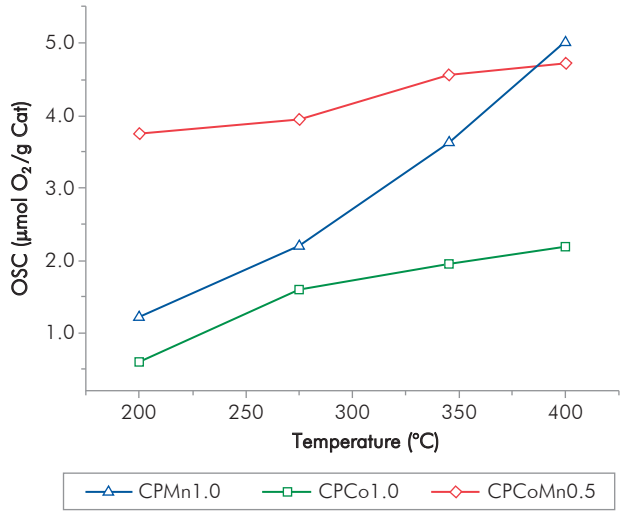

Figure 5. OSC of the mixed oxides at different temperatures.

The oxygen mobility of the oxides is an important factor in oxidation reactions given that if the oxygen species present sufficient mobility, the lattice oxygens can become involved in the catalytic process (Spivey, 1987; Yamazoe & Teraoka, 1990). The isotopic exchange technique provides information regarding oxygen mobility in terms of the exchange capacity of the oxygen species present in the materials. There are three routes by which the $^{18}O/^{16}O$ exchange can be undertaken (Nováková, 1971; Royer, Duprez & Kaliaguine, 2005) :

1. Homogeneous exchange: This reaction does not require the participation of the oxygen atoms of the solid and the concentrations of ^{16}O and ^{18}O remain constant during the test:

$$^{16}O_2(g) + {}^{18}O_2(g) \Leftrightarrow 2\,{}^{18}O^{16}O(g)$$

2. Simple heterogeneous exchange: Involves an oxygen atom of the oxide and an oxygen atom of the gaseous phase.

$$^{18}O^{18}O\,(g) + {}^{16}O(s) \Leftrightarrow {}^{18}O^{16}O(g) + {}^{18}O(s)$$

3. Multiple heterogeneous exchange: This mechanism involves the participation of two of the atoms of the solid in each step.

$$^{18}O^{18}O\,(g) + 2\,{}^{16}O(s) \Leftrightarrow {}^{16}O^{16}O(g) + 2\,{}^{18}O(s)$$

The variation of the concentrations of $^{16}O_2$, $^{16}O^{18}O$ and $^{18}O_2$ in the three oxides during the tests shows that the predominant exchange in these materials corresponds to the heterogeneous exchange (Figure 6).

A way of comparing exchange capacity among the materials and therefore oxygen mobility is in terms of the concentration of $^{16}O_2$, where the oxide which presents the greatest concentration of $^{16}O_2$ will be the solid with the greatest oxygen mobility. CPCo1.0 exhibits the highest concentrations of $^{16}O_2$ and therefore the greatest oxygen mobility at all oxides in the temperatures tested.

Ethyl acetate is a compound found in the paint, cosmetics, industrial dyes and is considered one of the most difficult molecules to oxidize in catalysts based on noble metals (Papaefthimiou, Ioannides & Verykios, 1997).

The curves of total conversion of ethyl acetate to CO_2 versus the reaction temperature are shown in Figure 7. Temperatures to reach 50% (T_{50}) and 90% (T_{90}) of conversion of VOC to CO_2 are employed as a measure of activity to compare the catalytic behavior among the catalysts. This figure shows the effect of the active phase, given that the oxides that contain manganese show better catalytic behavior than the single *Co* oxide. This behavior is explained in terms of the OSC results where the manganese oxides feature better redox properties (greater OSC values) than oxide CPCo1.0.

Table 1 lists the T_{90} values, the OSC, the concentration of the $^{16}O_2$ species and the quantity of α oxygen species desorbed at temperatures lower than 400°C. On the basis of these results, it can be established that high

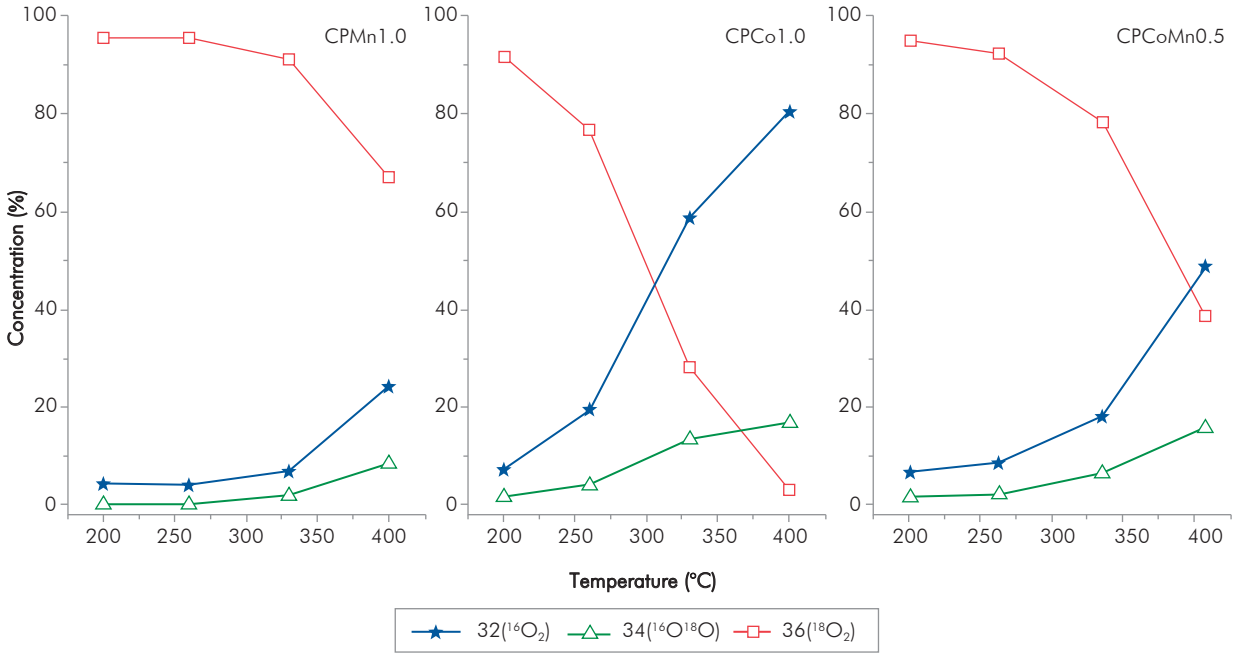

Figure 6. Isotopic exchange in *Mn* and/or *Co* mixed oxides. Adapted from (Castaño, Molina & Moreno, 2015).

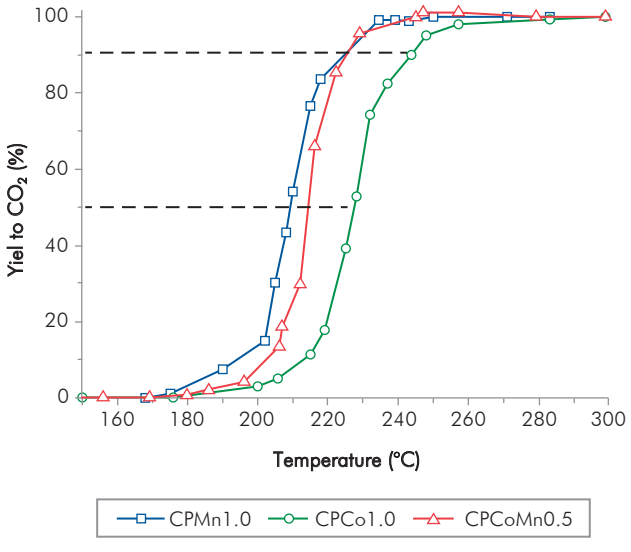

Figure 7. Catalytic performance of the mixed oxides in the total oxidation of ethyl acetate.

OSC values evidence the presence of more labile and reactive oxygen species capable of undergoing redox cycles and a high percentage of $^{16}O_2$ would show a great oxygen mobility.

In general, there is a relation between the catalytic activity and the OSC, where oxides CPMn1.0 and CPCoMn0.5 show the greatest oxygen storage capacity values and, therefore, is the catalyst with lower temperature to attain 90% conversion to CO_2.

5. RESULTS ANALYSIS

It is accepted in the literature that oxidation processes on oxides can be carried out by means of two mechanisms: suprafacial and intrafacial (Morales *et al*., 2007; Yamazoe & Teraoka, 1990; Zhang *et al*., 2012) . In the suprafacial mechanism the process is carried out at low temperatures (< 400°C) where the α adsorbed oxygen species play an important role in the catalytic activity, whereas in the intrafacial mechanism higher temperatures are required (> 400°C), which is also related to the redox properties and the mobility of oxygen species close to the surface and lattice oxygens represented like β species.

The presence of α and β species were determined by means of O_2-TPD, OSC and isotopic exchange techniques (these latter for β species) and their participation in the catalytic process was discussed with the T_{90} values in the oxidation of ethyl acetate.

Figure 7 and Table 1 show that mixed oxides CPMn1.0 and CPCoMn0.5 exhibit the same T_{90} value

Table 1. Correlation of the catalytic performance with the redox properties, oxygen mobility and oxygen species adsorbed on oxides.

Sample	$O_{2desorded}$ (α)[a] (μmol/g) T<400°C	Ethyl acetate		
		T_{90}[b] (°C)	OSC[c] (μmol/g)	$^{16}O_2$[d] (%)
CPMn1.0	2.7	226	2.6	24
CPCo1.0	1.1	240	1.2	80
CPCoMn0.5	0.5	226	4.0	48

[a] Quantity O_2 desorbed at temperatures below 400°C by O_2-TPD
[b] Temperature to reach 90% conversion to CO_2
[c] Oxygen Storage Capacity to T_{90}
[d] $^{16}O_2$ percentage to T_{90}

(226°C) even though with different quantity of oxygen species, different OSC and oxygen mobility values (Figures 4, 5 and 6). This similar catalytic activity among the manganese-containing oxides can be explained in terms of the participation of the α oxygen (oxygen adsorbed on the surface vacancies) in CPMn1.0 to compensate for the lower redox properties present in this oxide. On the other hand, CPCoMn0.5 has greater quantity of oxygens capable of produce redox cycles (greater OSC value), which are responsible for the oxidation process. Results suggest that in the oxidation of ethyl acetate on manganese mixed oxides, the participation of the surface adsorbed oxygens and the more labile oxygens participating in oxide-reduction cycles play a determining role possibly involving a suprafacial or intrafacial mechanism.

On the other hand, in oxide CPCo1.0 the catalytic behavior is essentially attributed to its high oxygen mobility, involving the participation of the bulk oxygens by means of an intrafacial mechanism. However, as shown in Table 1, even though this oxide presents the greatest oxygen mobility (represented by a greater quantity of $^{16}O_2$ exchanged) it is not necessarily the most active catalyst, therefore requiring the existence of optimum oxygen mobility and an acceptable capacity to participate in redox cycles or the presence of α oxygen species that participate in the oxidation reaction of VOCs.

From the results we can conclude that even though the three mixed oxides are derived from hydrotalcite type precursors, the oxygen species involved in the catalytic process depend on the oxygen vacancies generated, and the existent oxygen mobility, redox cycles and active phases.

6. CONCLUSION

The manganese-containing oxides (CPMn1.0 and CPCoMn0.5) show greater OSC values than the oxide containing single *Co* and therefore exhibit better catalytic behavior in the oxidation of the ester. The results demonstrated the joint participation of the adsorbed oxygens (α) and the redox properties of the oxides in the VOC oxidation given that even though CPMn1.0 (single manganese) shows lower redox properties than the *Co-Mn* oxide, the presence of a greater quantity of α species contribute to its catalytic behavior. The oxygen species involved in the catalytic process are dependent on the active phase employed, the oxygen vacancies, the oxygen mobility and the redox properties generated.

ACKNOWLEDGEMENTS

The authors thank DIB projects, Hermes codes 14785 and 15056 of *Universidad Nacional de Colombia.*

REFERENCES

Aguilera, D. A., Perez, A., Molina, R. & Moreno, S. (2011). *Cu–Mn* and *Co–Mn* catalysts synthesized from hydrotalcites and their use in the oxidation of VOCs. *Appl. Catal. B: Environ.,* 104(1-2), 144-150.

Arnone, S., Busca, G., Lisi, L., Milella, F., Russo, G. & Turco, M. (1998). Catalytic combustion of methane over $LaMnO_3$ perovskite supported on La_2O_3 stabilized alumina. A comparative study with Mn_3O_4, Mn_3O_4-Al_2O_3 spinel oxides. *Symposium (International) on Combustion*, 27(2), 2293-2299.

Avgouropoulos, G., Ioannides, T. & Matralis, H. (2005). Influence of the preparation method on the performance of CuO-CeO_2 catalysts for the selective oxidation of *CO*. *Appl. Catal. B: Environ*., 56(1-2), 87-93.

Bordeneuve, H., Guillemet-Fritsch, S., Rousset, A., Schuurman, S. & Poulain, V. (2009). Structure and electrical properties of single-phase cobalt manganese oxide spinels $Mn_{3-x}Co_xO_4$ sintered classically and by Spark Plasma Sintering (SPS). *J. Solid State Chem*., 182(2), 396-401.

Castaño, M. H., Molina, R. & Moreno, S. (2015). Cooperative effect of the *Co–Mn* mixed oxides for the catalytic oxidation of VOCs: Influence of the synthesis method. *Appl. Catal. A*, 492: 48-59.

Cavani, F., Trifirò, F. & Vaccari, A. (1991). Hydrotalcite-type anionic clays: Preparation, properties and applications. *Catal. Today,* 11(2), 173-301.

Christou, S. Y., García-Rodríguez, S., Fierro, J. L. G. & Efstathiou, A. M. (2012). Deactivation of $Pd/Ce_{0.5}Zr_{0.5}O_2$ model three-way catalyst by P, Ca and Zn deposition. *Appl. Catal. B: Envirn*., 111-112: 233-245.

Fierro, J. L. G. (2006). *Metal oxides: Chemistry and applications.* New York: CRC Press.

Garetto, T., Legorburu, I. & Montes, M. (2008). *Eliminación de emisiones atmosféricas de COVs por catálisis y adsorción.* Madrid: CYTED.

Jang, Y. I., Wang, H. & Chiang, Y. M. (1998). Room-temperature synthesis of monodisperse mixed spinel $(CoxMn_{1-x})_3O_4$ powder by a coprecipitation method. *J. Mater. Chem*., 8(12), 2761-2764.

Khan, F. I. & Ghoshal, A. (2000). Removal of volatile organic compounds from polluted air. *J. Losss Prevent. Proc*., 13(6), 527-545.

Koppmann, R. (2010). Chemistry of volatile organic compounds in the atmosphere. In: Timmis, K. (Ed.), *Handbook of hydrocarbon and lipid microbiology*. Berlín: Springer Berlin Heidelberg. 267-277.

Kovanda, F. & Jirátová, K. (2011). Supported layered double hydroxide-related mixed oxides and their application in the total oxidation of volatile organic compounds. *Appl. Clay Sci*., 53(2), 305-316.

Lamonier, J. F., Boutoundou, A. B., Gennequin, C., Pérez-Zurita, M., Siffert, S. & Aboukais, A. (2007). Catalytic removal of toluene in air over *Co–Mn–Al* nano-oxides synthesized by hydrotalcite route. *Catal. Lett*., 118(3), 165-172.

Li, Q., Meng, M., Xian, H., Tsubaki, N., Li, X., Xie, Y., Hu, T. & Zhang, J. (2010). Hydrotalcite-derived $Mn_xMg_{3-x}AlO$ catalysts used for soot combustion, NO_x storage and simultaneous soot-NO_x semoval. *Environ. Sci. Technol*., 44(12), 4747-4752.

Liotta, L. F., Ousmane, M., Di Carlo, G., Pantaleo, G., Deganello, G., Marcì, G., Retailleau, L., Giroir-Fendler, A. (2008). Total oxidation of propene at low temperature over Co_3O_4–CeO_2 mixed oxides: Role of surface oxygen vacancies and bulk oxygen mobility in the catalytic activity. *Appl. Catal*., A, 347(1), 81-88.

Liotta, L. F., Wu, H., Pantaleo, G. & Venezia, A. M. (2013). Co_3O_4 nanocrystals and Co_3O_4-MO_x binary oxides for *CO*, CH_4 and VOC oxidation at low temperatures: A review. *Catal. Sci. Technol*., 3(12), 3085-3102.

Mars, P. & van Krevelen, D. W. (1954). Oxidations carried out by means of vanadium oxide catalysts. *Chem. Eng. Sci*., 3(Supplement 1), 41-59.

Merino, N. A., Barbero, B. P., Grange, P. & Cadús, L. E. (2005). $La_{1-x}Ca_xCoO_3$ perovskite-type oxides: Preparation, characterisation, stability, and catalytic potentiality for the total oxidation of propane. *J. Catal*., 231(1), 232-244.

Mo, L., Fei, J., Huang, C. & Zheng, X. (2003). Reforming of methane with oxygen and carbon dioxide to produce syngas over a novel $Pt/CoAl_2O_4/Al_2O_3$ catalyst. *J. Mol. Catal. A: Chem*., 193(1-2), 177-184.

Morales, M. R., Barbero, B. P. & Cadús, L. E. (2007). Combustion of volatile organic compounds on manganese iron or nickel mixed oxide catalysts. *Appl. Catal. B: Environ.* 74(1-2), 1-10.

Moro-oka, Y., Ueda, W. & Lee, K. H. (2003). The role of bulk oxide ion in the catalytic oxidation reaction over metal oxide catalyst. *J. Mol. Catal. A: Chem*., 199(1-2), 139-148.

Muñoz, M., Moreno, S. & Molina, R. (2012). Synthesis of *Ce* and Pr-promoted *Ni* and *Co* catalysts from hydrotalcite type precursors by reconstruction method. *Int. J. Hydrogen Energy*, 37(24), 18827-18842.

Nováková, J. (1971). Isotopic exchange of oxygen ^{18}O between the gaseous phase and oxide catalysts. *Cat. Rev*., 4(1), 77-113.

Oyama, S. T. (1996). Factors affecting selectivity in catalytic partial oxidation and combustion reactions. In: Warren,

B. K. & Oyama, S. T. (Eds). *Heterogeneous hydrocarbon oxidation.* Washington: American Chemical Society. Vol. 638, Chapter 1, 2-19.

Papaefthimiou, P., Ioannides, T. & Verykios, X. E. (1997). Combustion of non-halogenated volatile organic compounds over group VIII metal catalysts. *Appl. Catal. B: Environ*., 13(3-4), 175-184.

Royer, S., Duprez, D. & Kaliaguine, S. (2005). Role of bulk and grain boundary oxygen mobility in the catalytic oxidation activity of $LaCo_{1-x}Fe_xO_3$. *J. Catal*., 234(2), 364-375.

Santos, V. P., Pereira, M. F. R., Órfão, J. J. M. & Figueiredo, J. L. (2009). Synthesis and characterization of manganese oxide catalysts for the total oxidation of ethyl acetate. *Top. Catal*., 52(5), 470-481.

Schwarz, J. A., Contescu, C. & Contescu, A. (1995). Methods for preparation of catalytic materials. *Chem. Rev.*, 95(3), 477-510.

Spivey, J. J. (1987). Complete catalytic oxidation of volatile organics. *Ind. Eng. Chem. Res*., 26(11), 2165-2180.

Tsai, Y. T., Mo, X., Campos, A., Goodwin Jr, J. G. & Spivey, J. J. (2011). Hydrotalcite supported *Co* catalysts for *CO* hydrogenation. *Appl. Catal. A*, 396(1-2), 91-100.

Tsyganok, A. & Sayari, A. (2006). Incorporation of transition metals into *Mg–Al* layered double hydroxides: Coprecipitation of cations vs. their pre-complexation with an anionic chelator. *J. Solid State Chem*., 179(6), 1830-1841.

Vaccari, A. (1998). Preparation and catalytic properties of cationic and anionic clays. *Catal. Today,* 41(1-3), 53-71.

Vedrine, J. C., Coudurier, G. & Millet, J. M. M. (1997). Molecular design of active sites in partial oxidation reactions on metallic oxides. *Catal. Today*, 33(1-3), 3-13.

Velu, S., Shah, N., Jyothi, T. M. & Sivasanker, S. (1999). Effect of manganese substitution on the physicochemical properties and catalytic toluene oxidation activities of *Mg–Al* layered double hydroxides. *Micropor. Mesopor. Mater*., 33(1-3), 61-75.

Wang, J., Shen, M., Wang, J., Gao, J., Ma, J. & Liu, S. (2011). CeO_2–CoO_x mixed oxides: Structural characteristics and dynamic storage/release capacity. *Catal. Today*, 175(1), 65-71.

Xu, Z. P., Zhang, J., Adebajo, M. O., Zhang, H. & Zhou, C. (2011). Catalytic applications of layered double hydroxides and derivatives. *Appl. Clay Sci*., 53(2), 139-150.

Xue, L., Zhang, C., He, H. & Teraoka, Y. (2007). Catalytic decomposition of N_2O over CeO_2 promoted Co_3O_4 spinel catalyst. *Appl. Catal. B: Environ*., 75(3-4), 167-174.

Yamazoe, N. & Teraoka, Y. (1990). Oxidation catalysis of perovskites- relationships to bulk structure and composition (valency, defect, etc.). *Catal. Today*, 8(2), 175-199.

Zhang, J., Weng, X., Wu, Z., Liu, Y. & Wang, H. (2012). Facile synthesis of highly active $LaCoO_3/MgO$ composite perovskite via simultaneous co-precipitation in supercritical water. *Appl. Catal. B: Environ*., 126:, 231-238.

Zhao, M., Shen, M. & Wang, J. (2007). Effect of surface area and bulk structure on oxygen storage capacity of $Ce_{0.67}Zr_{0.33}O_2$. *J. Catal*., 248(2), 258-267.

Zhu, L., Lu, G., Wang, Y., Guo, Y. & Guo, Y. (2010). Effects of preparation methods on the catalytic performance of $LaMn_{0.8}Mg_{0.2}O_3$ perovskite for methane combustion. *Chin. J. Catal.*, 31(8), 1006-1012.

AUTHORS

María-Haidy Castaño-Robayo
Affiliation: *Universidad Nacional de Colombia*
Chemist, *Universidad Nacional de Colombia*
Ph.D. in Chemical Sciences, *Universidad Nacional de Colombia*
e-mail: mhcastanor@unal.edu.co

Rafael Molina-Gallego
Affiliation: *Universidad Nacional de Colombia*
Chemist, *Universidad Nacional de Colombia*
Ph.D. in Applied Natural Sciences, *Université Catholique de Louvain*
e-mail: ramolinag@unal.edu.co

Sonia Moreno-Guáqueta
Affiliation: Universidad Nacional de Colombia
Chemist, Universidad Nacional de Colombia
Ph.D. in Applied Natural Sciences, *Université Catholique de Louvain*
e-mail: smorenog@unal.edu.co